Climate Dynamics (2001) 18: 321–330

C. C. Raible · U. Luksch · K. Fraedrich · R. Voss

North Atlantic decadal regimes in a coupled GCM simulation

Received: 15 September 2000 / Accepted: 30 March 2001

Abstract The non-stationarity of the North Atlantic atmosphere-ocean coupling is investigated utilizing a long time integration of a coupled atmosphere-ocean general circulation model (GCM) and a consistent atmospheric experiment forced by the climatological sea surface temperature (SST) of the coupled GCM. The temporal behavior of the North Atlantic Oscillation (NAO) is non-stationary with two different decadal regimes being identified: (a) phases with enhanced (active) low-frequency variability of the NAO index are characterized by *regional* modes with a baroclinic Pacific-North America (PNA) and a dominant barotropic North Atlantic pattern; (b) in phases with reduced (passive) low-frequency variability a *global* mode connects tropics and midlatitudes. The characteristic space scales are similar in the coupled and the consistent atmospheric experiment; the time scales of the atmospheric eigenmodes are modified by ocean dynamics. In the active (passive) phase the corresponding atmospheric mode is reinforced by the North Atlantic (tropical Pacific) SST.

1 Introduction

The North Atlantic Oscillation (NAO) plays an important role for the European climate and its variability (Hurrell 1995). It is characterized by the two anticorrelated "centers of action" of the Azores high and the Iceland low. They were identified a long time ago and used to define a circulation index (Defant 1924). During the last century the North Atlantic climate variability has covered a wide spectral band with a distinct low-frequency contribution; also proxy data of NAO show enhanced and reduced phases of low-frequency variability (Appenzeller et al. 1998).

The origin of low-frequency variability is still under debate ranging from external parameters like volcanos (Graf 1994), via internal (nonlinear) wave–wave interaction in the atmosphere (James and James 1989; James et al. 1994; Franzke et al. 2000) to stratosphere–troposphere coupling (Perlwitz et al. 2000). Furthermore, recent ensemble experiments show that the observed NAO variations are reproduced by a realistic SST forcing (Rodwell et al. 1999; Latif et al. 2000), but caution is needed when forced GCM simulations are used to interpret the variability of the coupled system. This is because the air–sea heat fluxes are of the reverse sign to those observed (Bretherton and Battisti 1999). In addition, atmosphere–ocean coupling and its impact are discussed in several observational and model studies, which often yield contradicting and confusing results (Frankignoul 1985; Lau 1997; Latif 1998).

Early observational studies of the North Atlantic climate (Bjerknes 1964) suggested a *regional mode* which describes the atmosphere–ocean interaction in terms of a conceptual model where the atmosphere leads the ocean on shorter and interannual time scales, while for longer time scales the ocean dynamics increases in importance. Recently, no difference between the wind–sea surface temperature relationship on interannual to interdecadal time scales have been identified, but a second mode has been found which may be forced by altered ocean currents rather than the local wind (Deser and Blackmon 1993). In addition Halliwell (1997) concluded that local atmospheric forcing of winter SST anomalies remains important for longer periods than previously realized. Using atmosphere–ocean general circulation models (GCM) a coupled mode has been identified in the North Pacific (Latif and Barnett 1994, 1996) and in the North Atlantic (Grötzner et al. 1998); the subpolar gyre reacts to wind field variations and the ocean is able to feed

C. C. Raible · U. Luksch (✉) · K. Fraedrich
Meteorologisches Institut,
Universität Hamburg, Germany
E-mail: luksch@dkrz.de

R. Voss
Deutsches Klimarechenzentrum Bundesstr. 55,
D-20146 Hamburg, Germany

back to the atmospheric fields. Timmermann et al. (1998) described a coupled oscillation between the NAO and the thermohaline circulation.

Observational studies emphasize the importance of tropical variations for the European climate suggesting a *global mode* of interaction between atmosphere and ocean (Rowntree 1972; Fraedrich and Müller 1992; Fraedrich 1994). For large warm (cold) SST anomalies in the eastern tropical Pacific the North Atlantic storm track tail is shifted southward (northward) leading to positive (negative) pressure anomalies over northern Europe and negative (positive) pressure anomalies over central Europe (Fraedrich and Müller 1992). Reversely, under low (high) pressure situations over central Europe, the North Pacific storm track extends less (further) eastward and thus closer (further) to the west coast of North America and a lack (occurrence) of a strong eastward stationary wave activity flux over the Atlantic (Fraedrich et al. 1993). This has been substantiated by GCM experiments reanalyzing the proposed El Niño Southern Oscillation (ENSO) Europe link (Palmer and Anderson 1995; May 1999; May and Bengtsson 1999).

Uncoupled atmospheric GCM experiments show that existing *atmospheric modes* are effectively reinforced by realistic North Atlantic SST anomalies (Robertson et al. 2000). The intensity of the quasi-barotropic atmospheric response is modified by baroclinic eddies (Peng and Whitaker 1999; Walter et al. 2000) showing an influence on the hemisphere scale. Blade (1997) noted that SST anomalies in the real world act to bias the atmospheric circulation toward certain flow regimes by increasing their persistence. On the synoptic scale weather regimes are defined either in terms of local density maxima in phase space or as areas of phase space where the state vector is quasi-stationary (Palmer 1999).

In an attempt to unify these different aspects we interpret the impact of regional and global ocean–atmosphere coupling as part of the non-stationary behavior of NAO and present a regional or global regime with enhanced or reduced low-frequency variability utilizing GCM experiments. A brief description of the atmosphere and ocean models, the experimental design, and the data analysis methods are introduced in Sect. 2. Then, characteristic spatial and time scales in a coupled atmosphere–ocean experiment are compared with observations and with an atmospheric simulation forced by climatological SST (Sect. 3). Decadal regimes are presented in Sect. 4. The results are summarized in Sect. 5.

2 Experimental design and analysis methods

An atmospheric and an ocean GCM are used to analyze the climate variability in the North Atlantic by two consistent experiments: (1) the atmosphere-ocean interaction is simulated by a coupled GCM and (2) the internal atmospheric dynamic is simulated as an atmospheric response forced by the consistent climatological SST which is prescribed by the coupled experiment.

2.1 Models

The fourth version of the *E*uropean *C*entre model of *Ham*burg (ECHAM-4) is the atmospheric part of the coupled general circulation model (Roeckner et al. 1996). This spectral model is used with triangular truncation at wave number 30 (T30), corresponding to a longitude–latitude grid of approximately $3.75° \times 3.75°$ and 19 hybrid sigma-pressure levels in the vertical up to 10 hPa. The T30-resolution is chosen as a good compromise between computational costs and realistically simulated climate statistics compared with ECMWF-Reanalyses (Stendel and Roeckner 1998).

The oceanic part of the coupled general circulation model is the *H*amburg *o*cean model in *p*rimitive *e*quations (HOPE) simplified by the Boussinesq approximation and formulated on a Gaussian T42 Arakawa-E grid (Wolff et al. 1997). The horizontal resolution is approximately $2.8° \times 2.8°$, whose meridional part is increased in the tropics to 0.5°. In the vertical the model consists of 20 irregularly distributed levels with ten levels in the first 300 m.

2.2 Experimental design

Two experiments are carried out: a coupled experiment which simulates the present day climate variability and identifies physical mechanisms of the atmosphere–ocean interaction and, for comparison, a consistent atmospheric experiment forced by a climatological boundary condition.

1. Coupled experiment: ECHAM-4 and HOPE are coupled through OASIS (Terray et al. 1998, *O*cean *A*tmosphere *S*ea *I*ce *S*oil) and an annual mean flux correction schemes for heat and fresh water; the atmospheric component, ECHAM-4, is modified compared to the standard version in order to account for sub-grid scale partial ice cover. A 600-year simulation for present-day climate conditions is carried out (Legutke and Voss 1999); the focus in this study lies on a period of 100 model-years. The first 130 years are not used because of a drift. Note that the model drift is mainly found in the Southern Hemisphere, so the influence on the Northern Hemisphere is weak.

2. Atmospheric experiment: SST, sea ice cover, sea ice thickness, and sea ice albedo of the coupled experiment are averaged over 100 years (a mean seasonal cycle January to December). These are the fixed boundary conditions for the atmospheric model ECHAM-4. A 100-year atomspheric simulation is carried out. Note that there is no bias in long term mean ocean and sea-ice components of both experiments. In this sense, the atmospheric experiment is consistent with the coupled experiment.

2.3 Data analysis techniques

Spatial patterns are identified by regional empirical orthogonal function (EOF) analysis of the 500 hPa geopotential in the Atlantic sector (20°N–69°N to 89°W–8°E) and the Pacific-North America sector (8°N–69°N to 180°W–60°W) analyzed in terms of the winter season means (December to February). The *temporal behaviour* of the first North Atlantic eigenmode (NAO) is discussed by spectral analysis of an index. For comparison with observations (Hurrell 1995) the NAO index in the simulations is defined as the normalized 500 hPa geopotential difference averaged over four points (near Azores minus Iceland). [NAO indices calculated for the simulated 500 hPa and the 1000 hPa geopotential are highly correlated, (correlation coefficient: 0.9).] The centered variance (deviation from the long term mean) on the 5 to 30-year spectral band of this index is used to define phases with enhanced ("active": ≥ one standard deviation) or reduced ("passive": ≤ – one standard deviation) variability. The variance of the 5 to 30-year spectral band is deduced for each 30-year window using the maximum entropy method. Note, that the identification of active and passive phases with this spectral method is insensitive using slightly different band-pass filters (4–30, 6–30, 5–25 years) or different lengths of the phases (25, 30 years). The total variance,

however, is comparable in both phases (using an *f*-test with a significance level 99%).

The non-stationarity of the space–time variability is described by different *regimes*. These regimes are identified by active and passive phases of the NAO index and the corresponding spatial scales utilizing global teleconnection maps. The maps are deduced for each 30-year phase by the teleconnectivity which is the strongest negative correlation of the 500 hPa geopotential at one base point with all grid points assigned at the base point (Wallace and Gutzler 1981). Only strong negative correlations which clustered together in a large area are considered as "centers of action". One-point correlation maps show the connection between these centers which are denoted by arrows.

3 Climatological setting

The characteristic space and time scales of the coupled experiment are compared (a) with observations to demonstrate that the model adequately represents the observed climate variability and (b) with the consistent atmospheric experiment (forced by the climatological SST of the coupled simulation) to illustrate the influence of interactive ocean dynamics. Non-stationarity in the space–time variability is described by phases of enhanced (active) or reduced (passive) low-frequency variability of the NAO.

3.1 Coupled experiment

The *spatial patterns* are presented by a regional EOF-analysis of the 500 hPa geopotential anomalies (using 100 model-years). The first EOF in the North Atlantic shows a NAO-like structure with two centers of action near the Azores and Greenland (Fig. 1). The second EOF displays a monopole structure, with its center extending from Great Britain to Iceland. The two EOFs explain 37% and 24% of the total variance, their spatial structures and explained variances resemble observational studies (Kutzbach 1970; Glowienka-Hense 1990; Zorita et al. 1992). Furthermore, the coupled model is also able to simulate the Pacific-North American circulation in a realistic way: The first EOF of the 500 hPa geopotential anomalies shows a PNA-like pattern (Fig. 1b, 46% of the total variance) and the second EOF (18%) is similar to the West Pacific pattern. Both EOFs correspond to observations (Wallace and Gutzler 1981; Wallace et al. 1993).

The *temporal behaviour* in the North Atlantic region is characterized by the NAO index and compared to last 100 years of observations (Hurrell 1995). The observed and simulated NAO vary on interannual up to interdecadal time scales (Fig. 2; thin: winter means; thick:

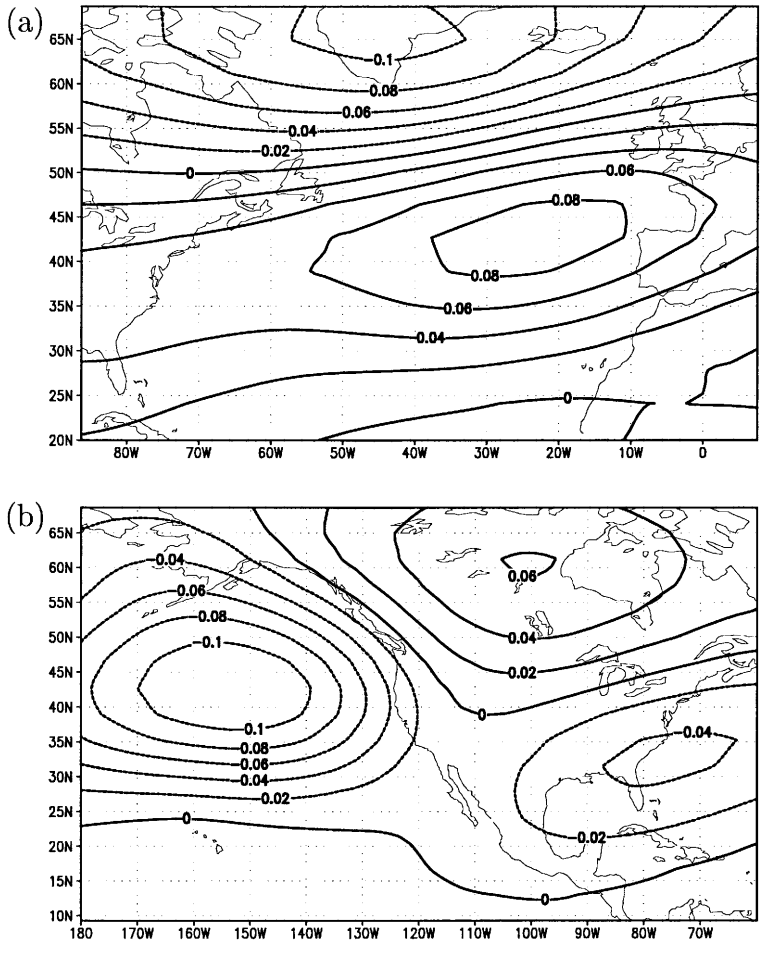

Fig. 1a, b Coupled experiment: first EOF patterns of 500 hPa geopotential (the model year from 130 to 229) for **a** North Atlantic and **b** Pacific-North America sector

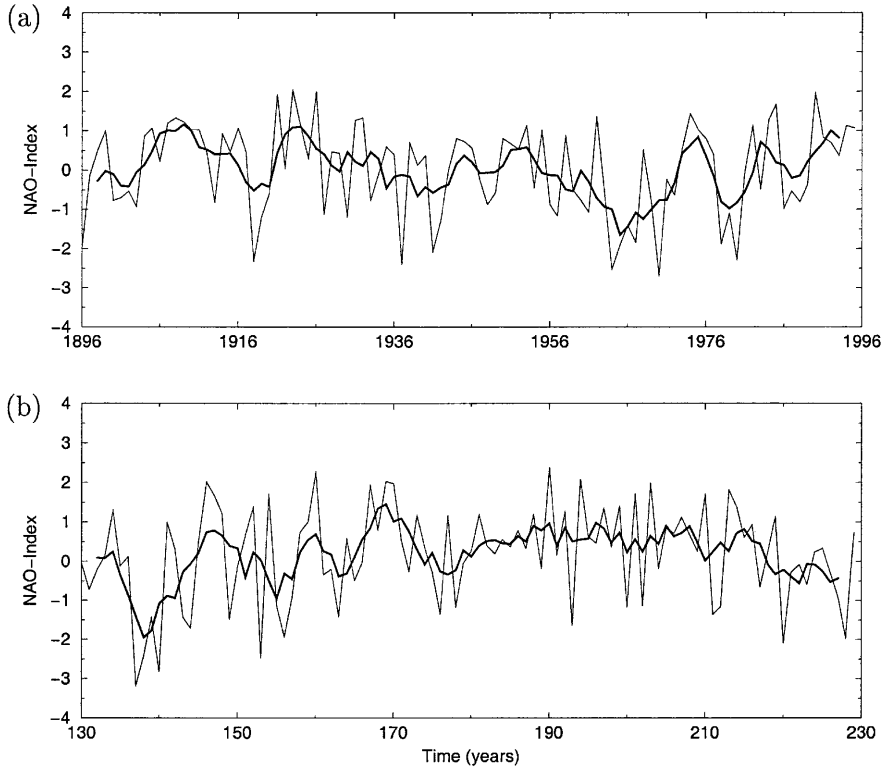

Fig. 2a, b Time series of the NAO-Index: **a** observations from 1896 to 1995 (Hurrell 1995) and **b** coupled experiment from model year 304 to 403. *Thin lines* represent winter means (December–February), *thick lines* show the 5-year running mean

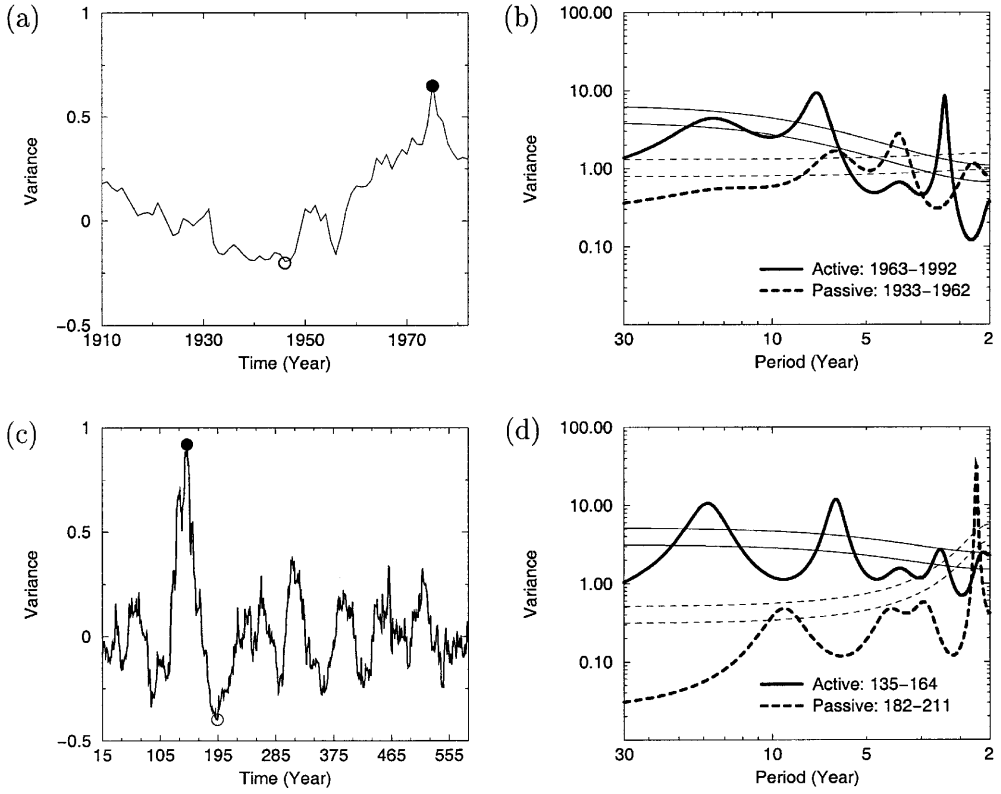

Fig. 3a–d The centered variance (deviation from the long term mean) of the 5 to 30 year spectral band and spectra of the unfiltered NAO index: **a**, **b** observation and **c**, **d** coupled experiment with *solid circles* (*open circles*) denoting active (passive) phases. Fitted AR(1)-processes and 95% confidence levels are included in **b**, **d** by *thin lines*

5-year running mean). Low-frequency variability is not dominant throughout the whole time series but only in certain phases. This indicates non-stationarity which can be quantified by spectral analysis (Fig. 3). The following results are noted: the centered variance of the 5 to 30-year spectral band (Fig. 3a, c) shows maxima (or active phases; dot) and minima (or passive phases; circle) in observations (active: 1963–1992, passive: 1933–1962)

and the coupled simulation (active: 135–164, passive: 182–211). The active phase is dominated by periods of 15 and 7 years analyzing the unfiltered observed (Fig. 3b) and the unfiltered simulated NAO index (Fig. 3d). Phases showing a minimum of low-frequency variability are characterized by enhanced variance on shorter time scales (observed: 4 year; simulated: 2.5 year period). The fitted AR(1) process and the 95% confidence level introduced for both phases (Fig. 3b, d) show that the temporal characteristic in these phases differs significantly, that is the NAO index behaves in a non-stationary manner. Both the observed and the simulated distribution of the NAO index is wider in the active than in the passive phase. This non-stationarity of the coupled experiment resembles the observational study (Appenzeller et al. 1998) using proxy data.

3.2 Atmospheric experiment

The characteristic space and time scales of the consistent atmospheric experiment with fixed SST and sea-ice distribution is compared with the coupled experiment to illustrate the effect of the internal atmospheric dynamics. The *spatial setting* of the 100-year atmospheric experiment is presented by a regional EOF-analysis applied to 500 hPa geopotential anomalies. In the North Atlantic the first atmospheric EOF shows a NAO mode (Fig. 4a; first and second EOF explain 39% and 27% of the total variance) whose structure, explained variance, and total variance resemble the coupled experiment. In the Pacific and North America region, the first EOF displays a PNA mode (Fig. 4b). The first and second EOF are responsible for 35% and 23% of the total variance. In this region the explained variance of the first EOF and the total variance is significantly reduced near the Aleutian low (99% significance level using an *f*-test), because ENSO-like variability is not included in this experiment.

The *temporal behaviour* of the NAO again shows interannual to decadal variability in both the atmospheric experiment (Fig. 5a) and the coupled experiment (Fig. 2a). Non-stationarity of the low-frequency variability can also be identified in terms of an active and a passive phase (active: 17–46, passive: 42–71, Fig. 5b). The distribution of the NAO index in the two phases behaves similar. However, the centered variance in the atmospheric experiment (Fig. 5b) is less enhanced for active phases and less reduced for passive phases than in both coupled experiment and observation. In the active phase, the dominant peak occurs at period of 10 years

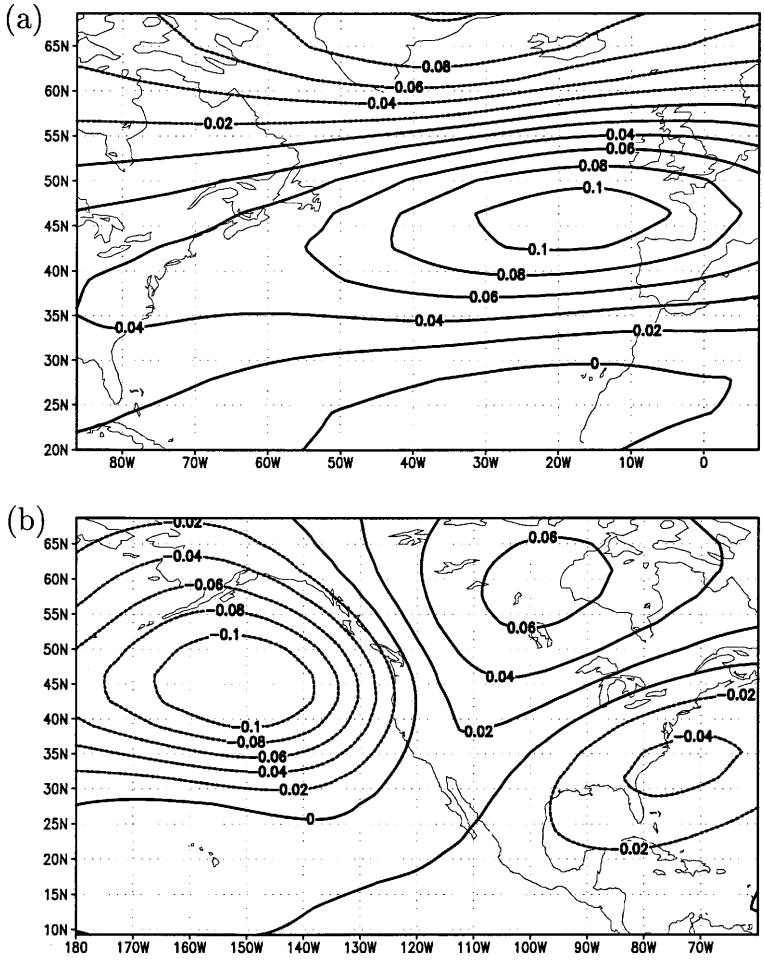

Fig. 4a, b As in Fig. 1 but for the atmosphere experiment

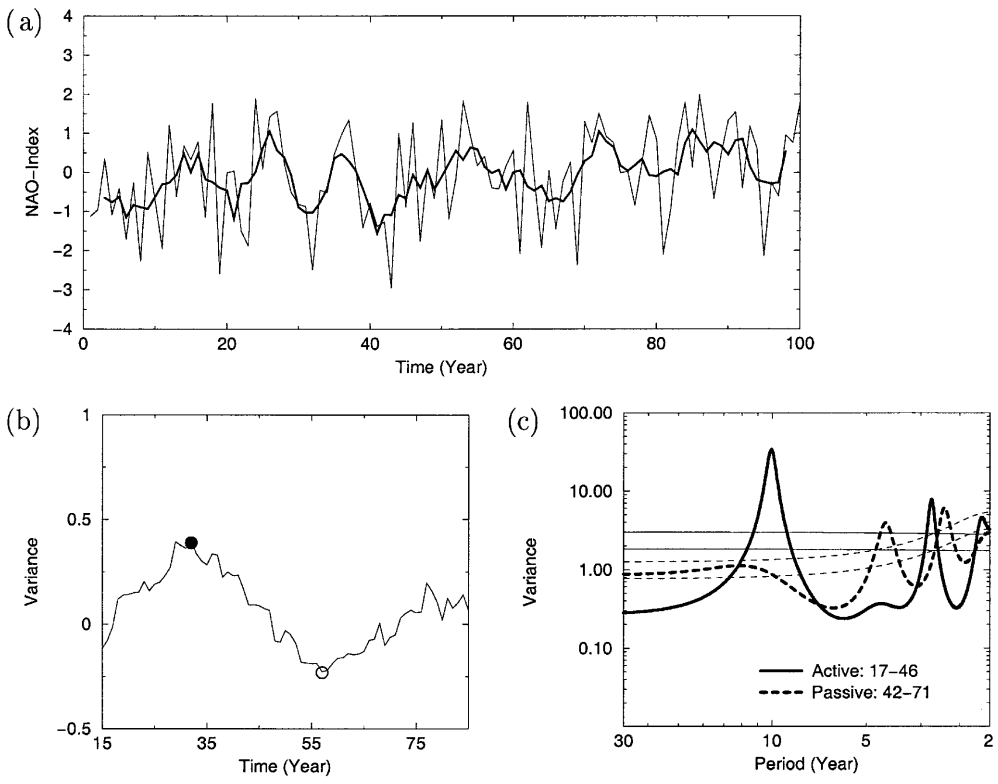

Fig. 5a–c Atmospheric experiment: **a** time-series of the NAO index, **b** the centered variance of the 5 to 30-year spectral band, and **c** the spectra of the unfiltered NAO index of the active (*solid circle*) and passive (*open circle*) phase. Fitted AR(1)-processes and 95% significance levels are included in **c** by *thin lines*

and in the passive phase only the period of 4 years is dominant (Fig. 5c).

In brief atmospheric dynamics are able to produce large-scale eigenmodes similar to observations, but ocean dynamics influence the temporal behavior of these eigenmodes. The characteristic space scales show a dipole structure in the North Atlantic and a tripole in the PNA region. However, the low-frequency variability of the NAO in the atmospheric experiment is less enhanced for active phases and less reduced for passive phases than in both the coupled experiment and the observation.

4 Decadal regimes

The non-stationarity of the space-time variability identified in the 100-year of both simulations is manifested by phases of enhanced (active) and reduced (passive) low-frequency variability of the NAO index (Sect. 3). Now, the spatial structure of these 30-year phases is separately analyzed by teleconnection maps identifying two different decadal regimes. To illustrate the corresponding ocean-atmosphere coupling the coupled simulation is compared with the consistent atmospheric experiment.

The *active regional regime* is characterized by two regional modes in the teleconnectivity pattern: a NAO and a PNA pattern (denoted by arrows in Fig. 6a). Comparing the teleconnectivity at 500 hPa with that at 1000 hPa the NAO has a barotropic structure. The PNA pattern is only found in the 500 hPa level, so it is a baroclinic mode, which is consistent to the observational study (Wallace and Gutzler 1981). The correlation maps between the NAO index (Fig. 7a) and the 500 hPa geopotential field as well as the corresponding SST show a regional structure (Fig. 7c, e) implying a regional atmosphere–ocean coupling. The correlation map between a high-pass filtered (< 5 years) NAO time series and the SST displays no significant correlations in the tropical Pacific region, so ENSO has no important influence. In the North Atlantic the correlation is reduced compared to the unfiltered case but the tripole structure remains. This reduction might be a pointer to the relevance of the regional atmosphere–ocean coupling. Whether the coupling in the active phase is a two-way interaction (Grötzner et al. 1998) or whether the ocean only integrates the atmospheric white noise (based on stochastic climate model concept; Hasselmann 1976) is still an open question. These results are compared with the teleconnectivity and local correlations of the consistent atmospheric experiment for the active phase. Here, an NAO pattern similar to the NAO mode in the coupled experiment is identified but no PNA pattern (not shown). The NAO centers are displaced eastwards and the signal especially of the southern center is not as distinct as in the coupled experiment. The correlation between the NAO index (Fig. 8a) and the 500 hPa geopotential field shows again a regional structure (Fig. 8c). Observational studies (Wallace and Gutzler 1981) analyzing the winter months from 1962 to 1976, which is in a phase of enhanced low-frequency variability, describe the regional modes similar to those of the coupled experiment. Moreover, the analysis of

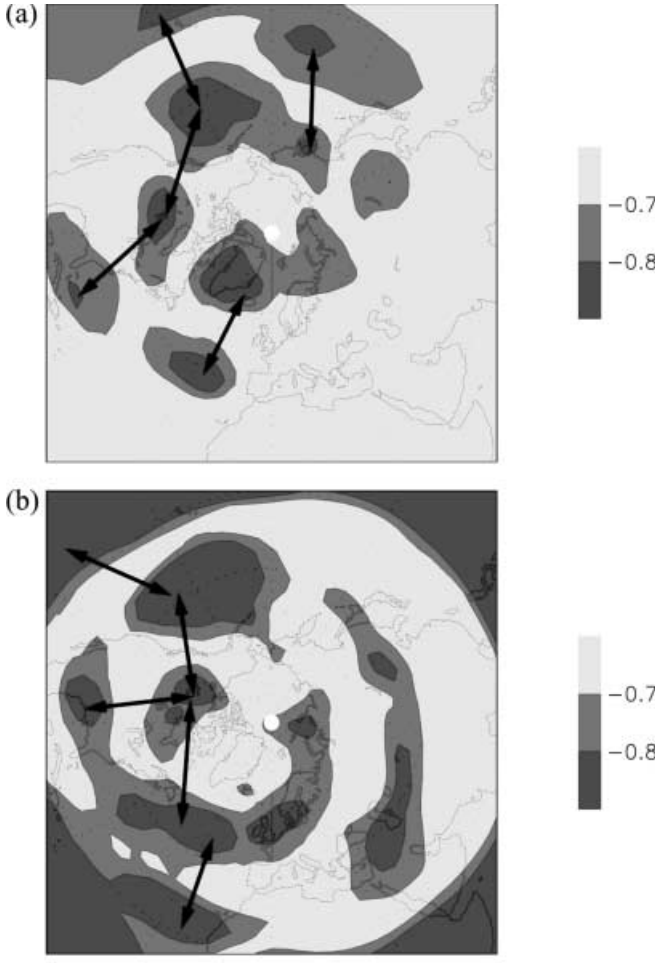

Fig. 6a, b Coupled experiment: teleconnectivity at 500 hPa geopotential (strongest negative correlation on each one-point correlation map) for **a** the active (year 135–164) and **b** the passive phase (year 182–211). *Arrows* show connections between the centers of action

NCEP data (using 1948–68 as passive and 1969–89 as active phase) shows similar correlation pattern to the coupled experiment in Fig. 7 (Walter and Graf submitted 2001).

The *passive global regime* is dominated by a PNA pattern identified by the teleconnectivity at 500 hPa (denoted by arrows in Fig. 6b) with a barotropic West Atlantic pole using also the teleconnectivity at 1000 hPa. The PNA is associated with large parts of the tropics and has a strong influence on the Atlantic region which is also displayed by correlation of the NAO index (Fig. 7b) and the 500 hPa geopotential (Fig. 7d). The NAO correlation with the global SST (Fig. 7f) shows low values in the North Atlantic region, but is large in the ENSO region where the explained variance reaches values of 49%. Observational and modelling studies (Zhang et al. 1996) show that the PNA pattern is connected to ENSO and that PNA can function as a link or 'bridge' between tropical and extratropical SST patterns in the Pacific. In the atmospheric experiment the teleconnectivity displays a baroclinic PNA mode which affects the Atlantic region (not shown). The correlation between the NAO index (Fig. 8b) and the 500 hPa geopotential field shows again a regional structure (Fig. 8d). However, the strong connection with the tropics is missing in the atmospheric experiment.

Thus, to sum up, the active regional regime is dominated by a regional ocean–atmosphere coupling in the North Atlantic and the passive global regime by a global ocean-atmosphere coupling with a strong impact from the tropics. Note that the total variance of the 500 hPa geopotential is comparable in the active and the passive phase of the coupled experiment (using an *f*-test with a significance level of 99%). The comparison of the coupled and the consistent atmospheric experiment demonstrates that the atmospheric dynamic already shows large-scale modes and non-stationary space–time variability but the intensity of the modes are influenced by ocean dynamics. Both regimes are also found in other active and passive phases of the 600-year coupled simulation (not shown). Moreover, the correlation between band-pass filtered (5 to 30-year period) 500 hPa geopotential and the NAO index of the whole 600-year simulation show a regional pattern whereas the correlation map of the high-pass filtered (>5-year) 500 hPa geopotential and the NAO index has a global structure.

5 Summary

Enhanced (active) and reduced (passive) low-frequency variability of the NAO describes the non-stationarity of midlatitude atmosphere-ocean coupling. This temporal behavior and the associated spatial scales are used to describe the decadal regimes utilizing a long time integration of a coupled atmosphere–ocean GCM and a consistent atmospheric simulation forced by climatological SST:

1. The *active* phase is characterized by two *regional* modes of the North Atlantic and the North Pacific. In the North Atlantic a barotropic NAO pattern dominates with centers near Iceland and the Azores which is correlated with the North Atlantic SST. In the North Pacific a baroclinic PNA mode is identified.
2. The *passive* phase is associated with a *global* mode with a dominant PNA pattern. Its Aleutian center is strongly linked to the tropics (ENSO) and to the North Atlantic region. The global correlation map of the NAO index and the SST shows high values in the tropical Pacific and low values in the North Atlantic sector.

The parts of the global and regional structures associated with the two regimes have so far been documented by observational and modelling studies. The *active regional regime* is characterized by the atmospheric eigenmode NAO correlated with the North Atlantic SST. In coupled GCM experiments two processes are presented as responsible for low-frequency variability: (a) a coupled atmosphere–ocean mode is identified where the ocean reacts on wind field variations and is able to feedback to the atmospheric fields (Grötzner et al. 1998);

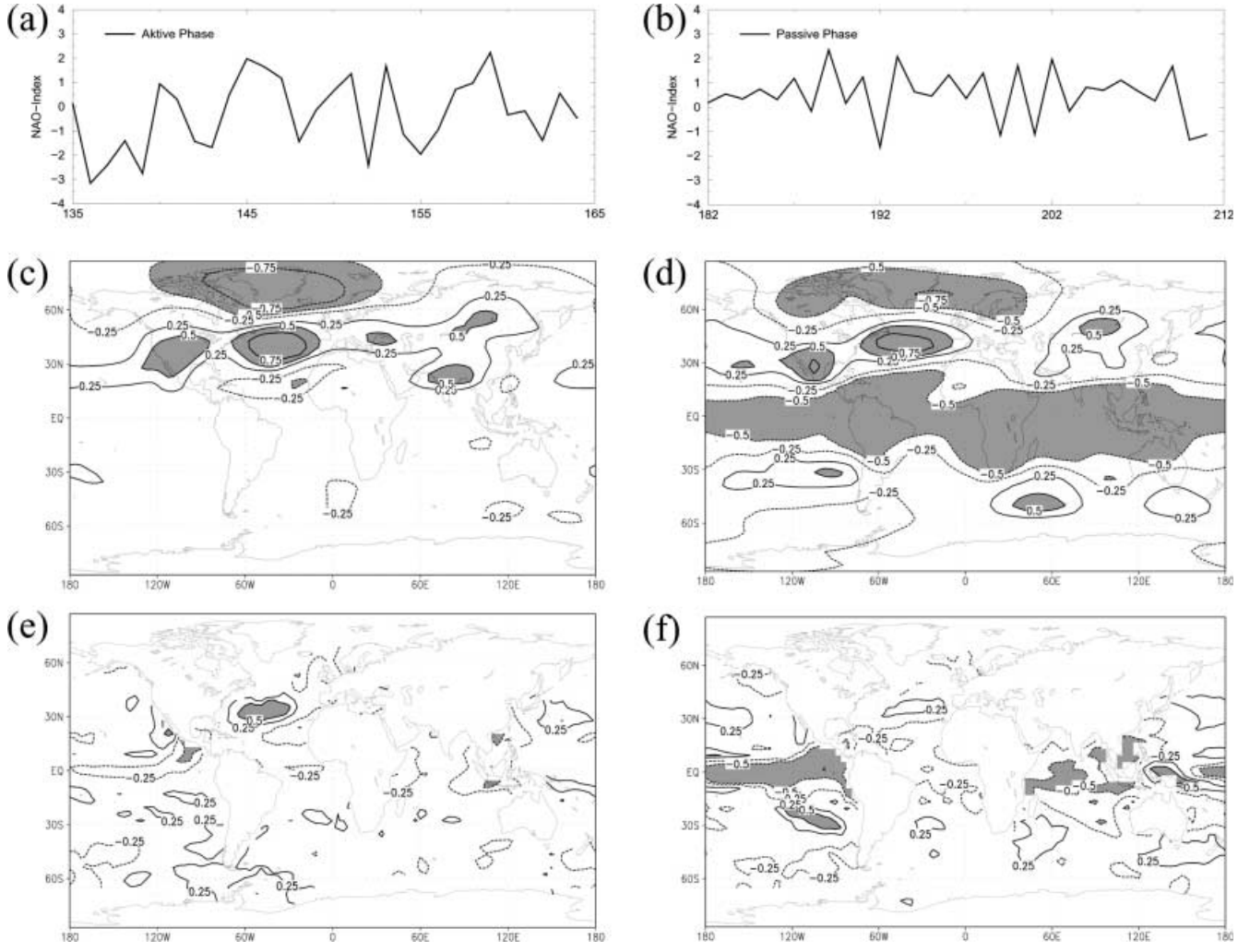

Fig. 7 Coupled experiment: **a**, **b** the NAO-index and **c**, **d** its correlation with the 500 hPa geopotential, and **e**, **f** with the sea surface temperature for the active regional (*left*) and the passive global regime (*right*); *shaded areas* are statistically significant at a level above 99%

(b) replacing the full ocean model with a 50 m fixed-depth mixed layer ocean shows that qualitatively similar power spectra are found compared to the coupled experiment with a complex ocean (Christoph et al. 1998). This suggests the subordinate relevance of a two-way atmosphere–ocean interaction in the North Atlantic and concludes that this coupled GCM experiment is mainly based on the stochastic climate model concept (Hasselmann 1976). Therefore, further GCM simulations coupled with a mixed layer ocean have to be employed to distinguish between one- and two-way coupling.

In the *passive global regime* a mode with a PNA structure and connections with the tropics and the North Atlantic is dominant and is correlated with the tropical Pacific SST. Observational studies which show an influence of ENSO on the European climate (e.g. Fraedrich 1994) are a manifestation of this regime. In this passive phase the energy flux from the Pacific to the Atlantic is important whereas in the active phase the regional atmosphere–ocean interaction in the North Atlantic sector is dominant. The relevance between passive (active) phase and the characteristic global (regional) spatial scales are also representative for other phases in the coupled experiment demonstrated by the correlation between a high-pass filtered (5–30 year band-pass filtered) NAO time series and the global 500 hPa geopotential field from a 600 year sample.

A discussion of the simulated non-stationarity of ocean-atmosphere coupling may be helpful for the understanding of the observed North Atlantic climate variability, because observations and simulations show several similarities. Firstly, a wavelet analysis of proxy data displays similar non-stationary temporal behavior (Appenzeller et al. 1998) as in the 600 year coupled simulation (not shown). Secondly, there is no coupling between Atlantic and Pacific in the active phase in the coupled experiment and in the observations over the last 30 years which are dominated by an active phase. Finally, the correlation coefficient between NAO and ENSO (defined by the Southern Oscillation index, Darwin minus Tahiti) increases from about zero in the active phase (last 30 years) to about 0.35 in the passive phase

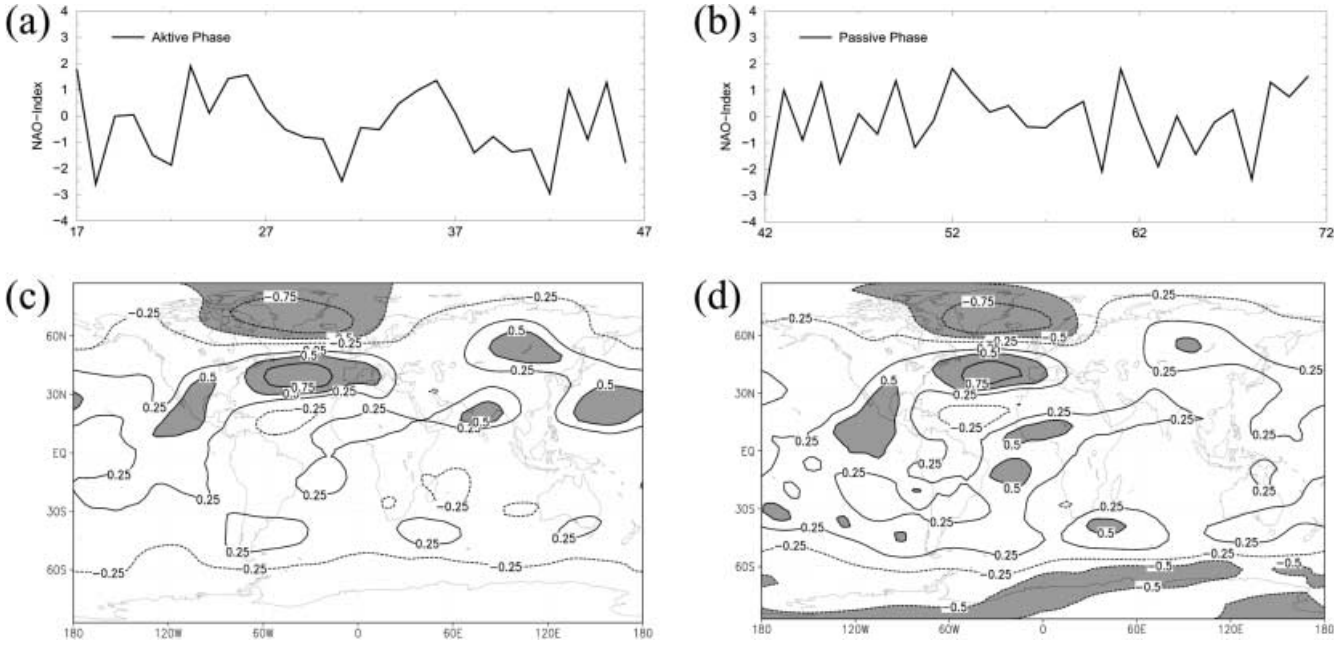

Fig. 8 Atmospheric experiment: **a**, **b** the NAO index and **c**, **d** its correlation with the 500 hPa geopotential of the active (*left*) and the passive phase (*right*); *shaded areas* are statistically significant at a level above 99%

(years 1933 to 1962). Although we assume that the simulated ENSO (measured as anomalous sea surface temperature of the Niño3-area, 5°N to 5°S, 170°W to 120°W) is artificially regular with a period of about two years (observations: 2–7 years), its impact on the global circulation is less relevant for the interpretation of the underlying mechanisms, because in the active phase ENSO shows no important influence on the North Atlantic.

The comparison of the coupled and the atmospheric experiment shows that the space scales are almost identical, but their temporal behavior is modified by the influence of ocean dynamics. Separation in time phases is required to identify the causes of the regional versus global atmosphere–ocean interaction. Furthermore, a mixed layer ocean model may be employed in further studies to separate the influence of large-scale ocean dynamics from the atmospheric induced anomalies in the mixed layer showing the contribution of the one- and two-way interaction in the active phase.

Acknowledgments Thanks are due to P. Sura, R. Blender, F. Lunkeit, and K. Walter for interesting discussions and U. Cubasch, and S. Legutke for providing the data of the coupled GCM simulation carried out by the Model Support Department at the *Deutsches Klimarechenzentrum*. This work is supported by the *Deutsche Forschungsgesellschaft* (SFB 512: "Tiefdruckgebiete und Klimasystem des Nordatlantiks").

References

Appenzeller C, Stocker TF, Anklin M (1998) North Atlantic oscillation dynamics recorded in Greenland ice cores. Science 282: 446–449

Bjerknes J (1964) Atlantic air–sea interaction. Adv Geophys 10: 1–82

Blade I (1997) The influence of midlatitude ocean/atmosphere coupling on the low-frequency variability of a GCM. Part I: no tropical SST forcing. J Clim 10: 2087–2106

Bretherton CS, Battisti DS (1999) An interpretation of the results from atmospheric general circulation models forced by the time history of the observed sea surface temperature distribution. Geophy Res Lett 27: 767–779

Christoph M, Ulbrich U, Oberhuber JM, Roeckner E (1998) The role of ocean dynamics for low-frequency fluctuations of the NAO in a coupled ocean-atmosphere GCM. Techn Rep 285, Max-Planck-Institut, Hamburg, Germany

Defant A (1924) Die Schwankungen der atmosphärischen Zirkulation über dem nordatlantischen Ozean im 25-jährigen Zeitraum 1881-1905. Geogr Ann 6: 13–41

Deser C, Blackmon ML (1993) Surface climate variations over the North Atlantic ocean during winter: 1900–1989. J Clim 6: 1743–1753

Fraedrich K (1994) An ENSO impact in Europe? A review. Tellus 46: 541–552

Fraedrich K, Müller K (1992) Climate anomalies in Europe associated with ENSO extremes. Int J Climatol 12: 25–31

Fraedrich K, Bantzer C, Burkhardt U (1993) Winter climate anomalies in Europe and their associated circulation at 500 hPa. Clim Dym 8: 161–175

Frankignoul C (1985) Sea surface temperature anomalies, planetary waves and air-sea feedback in the middle latitudes. Rev Geophys 23: 357–390

Franzke C, Lunkeit F, Fraedrich K (2000) Low-frequency variability in a simplified atmospheric GCM: stormtack induced 'spatial resonance'. Q J R Meteorol Soc 126: 2691–2708

Glowienka-Hense R (1990) The North Atlantic oscillation in the Atlantic-European SLP. Tellus 42: 497–507

Graf HF (1994) Northern Hemisphere tropospheric mid-latitude circulation after violent volcanic eruptions. Contrib Atmos Phys 67: 3–13

Grötzner A, Latif M, Barnett TP (1998) A decadal cycle in the North Atlantic ocean as simulated by the ECHO coupled GCM. J Clim 11: 831–847

Halliwell GR (1997) Decadal and multidecadal North Atlantic SST anomalies driven by standing and propagating basin-scale atmospheric anomalies. J Clim 10: 2405–2411
Hasselmann K (1976) Stochastic climate models Part I. Theory. Tellus 28: 473–484
Hurrell JW (1995) Decadal trends in the North Atlantic oscillation: regional temperatures and precipitation. Science 269: 676–679
James IN, James PM (1989) Ultra-low-frequency variability in a simple atmospheric circulation model. Nature 342: 53–55
James PM, Fraedrich K, James IN (1994) Wave-zonal-flow interaction and ultra-low-frequency variability in a simplified global circulation model. Q J R Meteorol Soc 120: 1045–1067
Kutzbach JE (1970) Large-scale features of monthly mean northern hemisphere anomaly maps of sea-level pressure. Mon Weather Rev 98: 708–716
Latif M (1998) Dynamics of interdecadal variability in coupled ocean-atmosphere models. J Clim 11: 602–624
Latif M, Barnett TP (1994) Causes of decadal climate variability over the North Pacific and North America. Science 266: 634–637
Latif M, Barnett TP (1996) Causes of decadal climate variability over the North Pacific and North America: dynamics and predictability. J Clim 9: 2407–2423
Latif M, Arpe K, Roeckner E (2000) Oceanic control of decadal North Atlantic sea level pressure variability in winter. Geophys Res Lett 27: 727–730
Lau NC (1997) Interactions between global SST anomalies and the midlatitude atmospheric circulation. Bull Am Meteorol Soc 78: 21–33
Legutke S, Voss R (1999) The Hamburg atmosphere-ocean coupled circulation model ECHO-G. Technical Report 18, Deutsches Klimarechenzentrum
May W (1999) Space-time spectra of atmospheric interseasonal variablity in the extratropics and their dependency on the El Nino/Southern Oscilation phenomenon: model versus observation. Clim Dym 15: 369–387
May W, Bengtsson L (1999) The signature of ENSO in the Northern Hemisphere midlatitude seasonal mean flow and high-frequency intraseasonal variability. Meteorol Atmos Phys 69: 81–100
Palmer TN (1999) A nonlinear dynamical perspective on climate prediction. J Clim 12: 575–591
Palmer TN, Anderson DLT (1995) The prospects for seasonal forecasting – a review paper. Q J R Meteorol Soc 121: 317–342
Peng S, Whitaker JS (1999) Mechanisms determining the atmospheric response to midlatitude SST anomalies. J Clim 12: 1393–1408
Perlwitz J, Graf HF, Voss R (2000) The leading variability mode of the coupled troposphere stratosphere winter circulation in different climate regimes. J Geophys Res 105: 6915–6926
Robertson AW, Mechoso CR, Kim YJ (2000) The influence of Atlantic sea surface temperature anomalies on the North Atlantic Oscillation. J Clim 13: 122–138
Rodwell MJ, Rowell DP, Folland CK (1999) Oceanic forcing of the wintertime North Atlantic oscillation and European climate. Nature 398: 320–323
Roeckner E, Arpe K, Bengtsson L (1996) The atmospheric general circulation model ECAHM-4: model description and simulation of present-day climate. Technical Report 218, Max-Planck-Institut
Rowntree PR (1972) The influence of tropical East Pacific ocean temperatures on the atmosphere. Q J R Meteorol Soc 98: 290–321
Stendel M, Roeckner E (1998) Impacts of the horizontal resolution on simulated climate statistics in ECHAM 4. Technical Report 253, Max-Planck-Institut
Terray L, Valcke S, Piacentini A (1998) The OASIS coupler user guide, version 2.2. Technical Report TR/CMGC/98-05, CERFACS: 77 pp
Timmermann A, Latif M, Voss R, Grötzner A (1998) North Atlantic interdecadal variability: a coupled air-sea mode. J Clim 11: 1906–1931
Wallace JM, Gutzler DS (1981) Teleconnections in the geopotential height field during the Northern Hemisphere winter. Mon Weather Rev 109: 782–812
Wallace JM, Zhang Y, Lau KH (1993) Structure and seasonality of interannual and interdecadal variability of the geopotential height and temperature fields in the Northern Hemisphere troposphere. J Clim 6: 2063–2082
Walter K, Luksch U, Fraedrich K (2000) A response climatology to idealized midlatitude thermal forcing experiments with and without a stormtrack. J Clim 9 (in press)
Wolff JO, Maier-Reimer E, Legutke S (1997) The Hamburg ocean primitive equation model HOPE. Technical Report 13, Deutsches Klimarechenzentrum
Zhang Y, Wallace JM, Iwasaka N (1992) Is climate variability over the North Pacfic a linear response to ENSO? J Clim 9: 1468–1478
Zorita E, Kharin V, von Storch H (1992) The atmospheric circulation and sea surface temperature in the North Atlantic area in winter: their interaction and relevance for the Iberian precipitation. J Clim 5: 1097–1108